

# Calibration of geometric distortion in the ACS detectors

Gerhardt R. Meurer<sup>a</sup>, Don Lindler<sup>b</sup>, John Blakeslee<sup>a</sup>, Colin Cox<sup>c</sup>, Andre Martel<sup>a</sup>, Hien Tran<sup>a</sup>, Rychard Bouwens<sup>d</sup>, Holland Ford<sup>a</sup>, Mark Clampin<sup>c</sup>, George Hartig<sup>c</sup>, Marco Sirianni<sup>a</sup>, and Guido deMarchi<sup>c</sup>

<sup>a</sup>Johns Hopkins University; <sup>b</sup>Sigma Science; <sup>c</sup>Space Telescope Science Institute; <sup>d</sup>University of California, Santa Cruz;

## ABSTRACT

The off-axis location of the Advanced Camera for Surveys causes strong geometric distortion in all detectors – the Wide Field Camera (WFC), High Resolution Camera (HRC), and Solar Blind Camera (SBC). Dithered observations of rich star cluster fields are used to calibrate the distortion. We describe the observations obtained, the algorithms used to perform the calibrations and the accuracy achieved. We present our best current calibration of the geometric distortion of each of the detectors.

Keywords: HST, ACS, WFC, HRC, SBC

## 1. INTRODUCTION

Images from the Hubble Space Telescope (HST) Advanced Camera for Surveys (ACS)<sup>1</sup> suffer from strong geometric distortion: the square pixels of its detectors project to trapezoids of varying area across the field of view. The tilted focal surface with respect to the chief ray is the primary source of distortion of all three ACS detectors: the Wide Field Camera (WFC), High Resolution Camera (HRC), and Solar Blind Camera (SBC). In addition, The HST Optical Telescope Assembly induces distortion as does the ACS M2 and IM2 mirrors (which are designed to remove HST's spherical aberration). The SBC's optics include a photo-cathode and micro-channel plate which also induce distortion.

Here we describe our method of calibrating the geometric distortion using dithered observations of star clusters and present the initial results of the calibration campaign.

## 2. OBSERVATION PLAN

The ACS geometric distortion campaign was comprised of two HST observing programs: 9028 which consisted of observations of the core of 47 Tucanae (NGC 104) with the WFC and HRC, and 9027 which consisted of SBC observations of NGC 6681. Additional observations from programs 9011, 9018, 9019, and 9024 were used as additional sources of data, to check the results, and to constrain the absolute pointing of the telescope. A full list of the field centers used is given in Table 1.

The CCD exposures of 47 Tucanae were designed to well detect stars on the main sequence turn-off at  $m_B = 17.5^2$  in each frame. This allows for a high density of stars with relatively short exposures. The F475W filter (Sloan  $g'$ ) was used for the CCD observations so as to minimize the number of saturated red giant branch stars in the field. For the HRC, which has very little observing time overheads, the data were obtained in two 60s exposures at each dither position, thus allowing easy cosmic ray rejection. The telescope time for short exposure WFC data is dominated by overheads, hence only a single 60s exposure was obtained at each dither position. Simulations of the HRC and WFC images made prior to launch were used to check that crowding would not be an issue. In addition we examined archival WFPC2 data of 47 Tuc from the datasets described by Gilliland et al.<sup>2</sup> Figures 1a,b show subsections near the cluster center of the WFC and HRC observations of 47 Tuc, confirming that the observations are not overly crowded.

Table 1. Observing programs and pointing centers.

Program	Camera	Filter	target	RA [J2000]	Dec[J2000]
9011	WFC,HRC	F550M, F502N	NGC188	00:47:04.54	+85:16:32.7
9028	WFC,HRC	F475W	47 Tuc	00:24:05.05	-72:04:50.0
9018	WFC	F775W	47 Tuc (6' W)	00:22:37.20	-72:04:14.0
9019	HRC	F775W	47 Tuc	00:24:06.52	-72:05:00.6
9019	HRC	F220W	NGC6681	18:43:12.67	-32:17:26.3
9024,9027	SBC	F125LP	NGC6681	18:43:12.67	-32:17:26.3

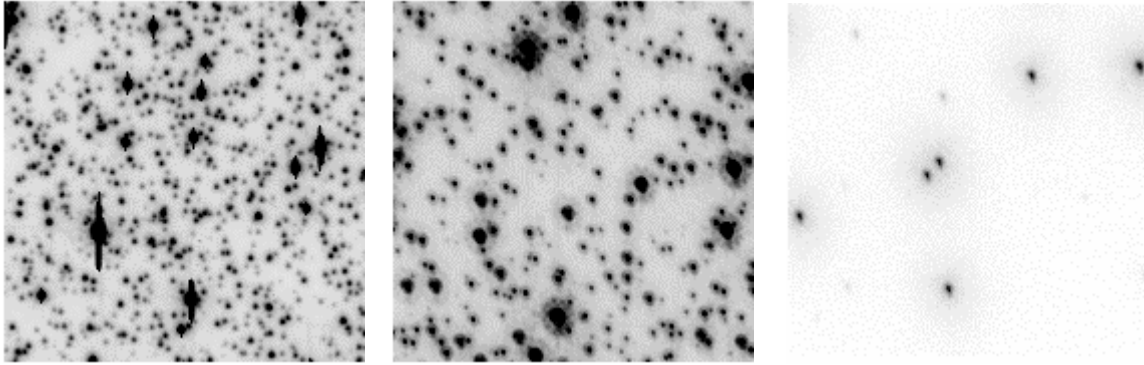


Figure 1. Subsections of images used for calibrating geometric distortion. From left to right: a. WFC F475W image of the center of 47 Tuc; b. HRC F475W image of the same field; c. SBC F125LP observation of the center of NGC6681. All subsections are 180 pixels on a side.

The SBC observations of NGC 6681 consisted of 450s exposures with the F125LP. NGC 6681 was chosen as the target due to the relatively high density of UV emitting hot horizontal branch stars. While the density of stars is sparse compared to the optical 47 Tuc observations, as shown in Fig. 1c, there are still over ten times more constraints than free parameters in the fits described below.

The pointing center was dithered around each star field. Figure 2 shows the pattern of offsets that were used for the WFC. This pattern, and that chosen for the HRC observations, were designed so that the offsets between all pairs of images adequately, and non-redundantly, samples all spatial scales from about 5 pixels to  $\frac{3}{4}$  the detector size. For the SBC observations, a more regular pattern of offsets is used augmented by a series of  $\sim 5$  pixel offsets. All pointings are done with POS TARG commands.

### 3. METHOD

#### 3.1 Distortion model

The heart of the distortion model relates pixel position  $(x,y)$  to sky position is a polynomial transformation given by:

$$x_c = \sum_{m=0}^k \sum_{n=0}^m a_{m,n} (x - x_r)^n (y - y_r)^{m-n} , \quad y_c = \sum_{m=0}^k \sum_{n=0}^m b_{m,n} (x - x_r)^n (y - y_r)^{m-n} \quad (eq.1)$$

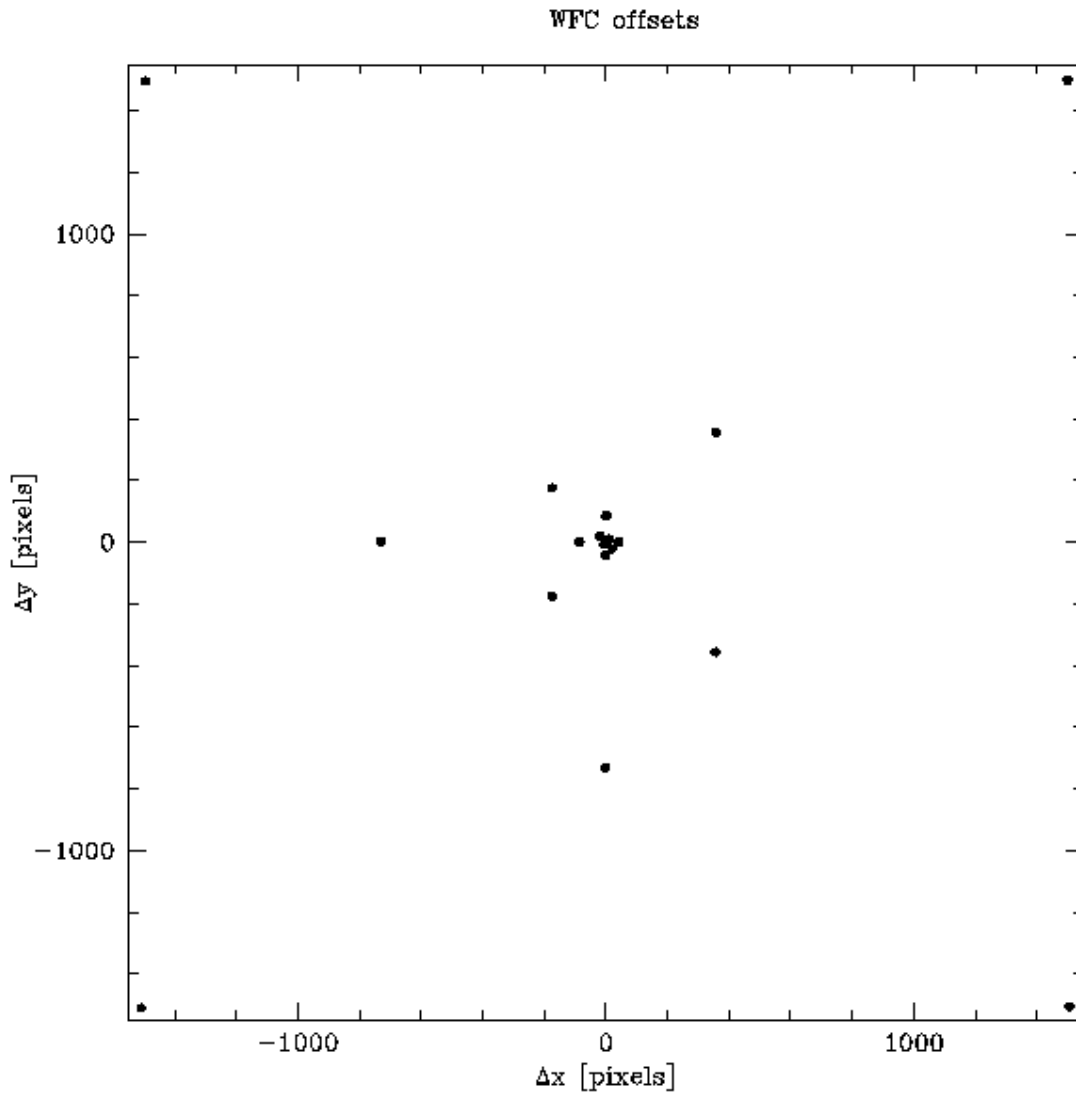


Figure 2. Pointing offsets used for WFC in program 9028.

Here  $x, y$  are display pixel positions relative the first pixel 1,1, and  $x_r, y_r$  is the reference pixel, taken to be the center of each detector, or WFC chip and  $x_c, y_c$  are undistorted image coordinates. The coefficients to the fits,  $a_{m,n}$  and  $b_{m,n}$ , are free parameters. To get to sky positions requires two more transformations. First, for the WFC, an offset is applied to get the two CCD chips on the same coordinate system:

$$X = x_c + \Delta x(\text{chip}\#) , Y = y_c + \Delta y(\text{chip}\#). \quad (\text{eq. 2})$$

$\Delta x(\text{chip}\#)$ ,  $\Delta y(\text{chip}\#)$  are 0,0 for WFC's chip #1 (as indicated by the CCDCHIP keyword in WFC FITS image headers) and correspond to the separation between chips 1 and 2 for chip #2. These offsets are free parameters in our distortion model fit. These offsets are not needed for the HRC and SBC. Finally, we must transform to tangential plane position on the sky  $X_{sky}, Y_{sky}$  :

$$X_{sky} = \cos \Delta\theta_i * X - \sin \Delta\theta_i * Y + \Delta X_i, \quad Y_{sky} = \sin \Delta\theta_i * X + \cos \Delta\theta_i * Y + \Delta Y_i, \quad (eq. 3)$$

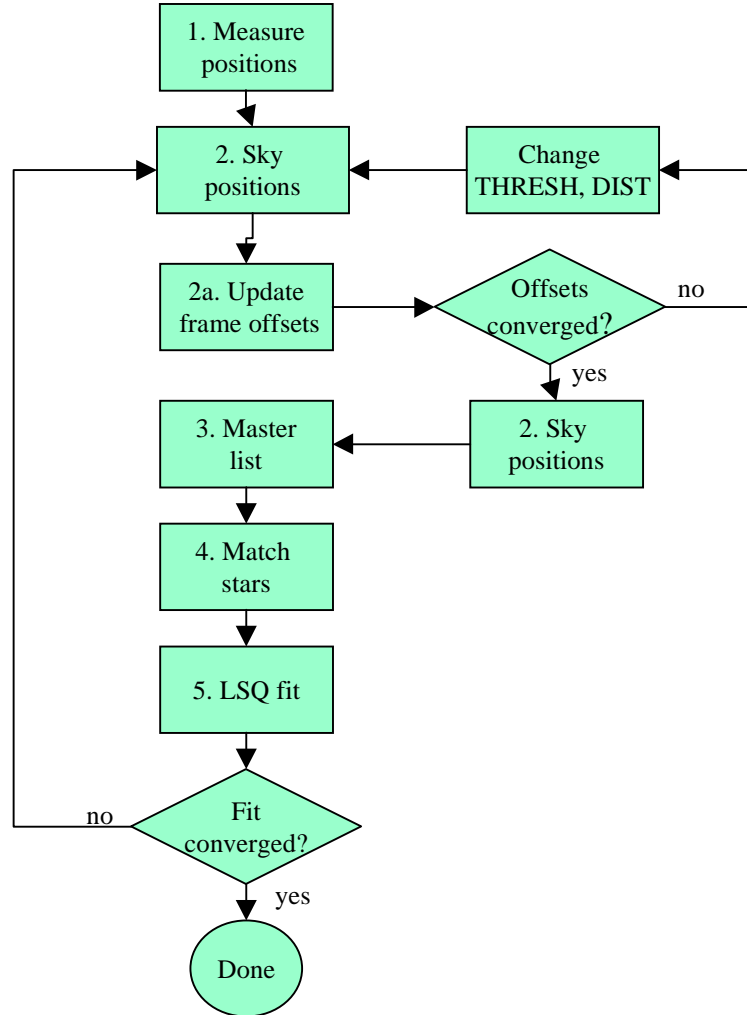
Where  $\Delta X_i$ ,  $\Delta Y_i$ ,  $\Delta\theta_i$  are the position and rotation offsets of frame  $i$ .

### 3.2 Calibration algorithm

We do an iterative solution to determine the following: the distortion coefficients  $a_{m,n}$ ,  $b_{m,n}$ ; the offset between the two WFC CCD chips  $\Delta x(chip \#)$ ,  $\Delta y(chip \#)$ ; the offsets of each frame  $\Delta X_i$ ,  $\Delta Y_i$ ,  $\Delta\theta_i$ ; and the tangential plane position  $X_{sky}$ ,  $Y_{sky}$  of each star used in the fit. The solution is done in the following steps

1. **Determine star positions on each frame.** This step only needs to be performed once for each frame. The algorithm used finds all local maxima above a specified threshold after smoothing by 3x3 box car filter. A 7x7 box around each local maxima is extracted, and the centroid is computed (after subtraction of 30% of the maximum and clipping at 0 so as to remove PSF wings), and compared to Gaussian fits to the  $x,y$  profiles. If the Gaussian and centroid positions differ by more than 0.25 pixels, or either the centroid or Gaussian position differ from the position of the local maximum by  $>1$  pixel then the measurement is rejected – the measurement is likely to be effected by crowding or a cosmic ray hit. For the measurements that are accepted, the Gaussian profile fit positions are used in the model fit.
2. **Compute sky positions for each measurement.** Use the current distortion solution and frame offsets and equations 1-3 to do the computation.
  - a. **Update of image offsets and orientation.** This optional step matches stars between each observation and the first observation. The user specifies a threshold and a search distance for matching. The difference in position of each star is determined and the median difference of all stars in a frame is taken as the frame offsets  $\Delta X_i$ ,  $\Delta Y_i$ . If requested, the orientation offset  $\Delta\theta_i$  is determined from a least squares fit to  $X_{sky}$  offset versus  $Y_{sky}$  and  $Y_{sky}$  offset versus  $X_{sky}$ . If step 2a is performed, step 2 should be repeated.
3. **Create master list of unique stars.** This step is done on each image that is fit in turn, with the first image chosen to be the central most pointing. A peak flux per pixel threshold and maximum search distance are specified. In a given image, if two stars are above the threshold within the same search distance, both are ignored. Except for these stars, all stars in the first image above the threshold are put on to the master list. Each subsequent image is then matched to the master list, using the current coefficients and image offsets. Stars above the peak threshold level that are not matched are added to the list. In the initial iterations of the fit, the search distance is set to be large (at least a few pixels), as is the threshold, so that only the brightest stars are matched. The result of this processing step is a list of  $X_{sky}$ ,  $Y_{sky}$  for each unique star.
4. **Match stars from each image to stars in the master list.** Using the current fit coefficients, then for a given peak flux threshold and matching distance (not necessarily the same used in step 3) the star positions are matched to the master list of unique stars produced in step 3. This results in a catalog of coordinates (raw and sky) linked with identifiers for the unique star, image, and chip.
5. **Least squares fit to determine new coefficients.** The distortion coefficients, chip offsets, image position and orientation offsets (with respect to the first image) are fit simultaneously in a least squares fit which minimizes the difference in the computed  $X_{sky}$ ,  $Y_{sky}$  and the average  $X_{sky}$ ,  $Y_{sky}$  for each unique star. The offsets of three images are not included in this fit: the first image in the list which acts as the fiducial image, and two images with large, approximately orthogonal offsets. The offsets of these images set the linear terms. They are selected to have the largest offsets with respect to the fiducial frame, with the constraint that all three images are obtained without changing guide stars.

Each of the above steps are implemented as IDL procedures. The steps are run in the order shown in Fig. 3. As shown, there are two places for the user to check convergence; first in an inner loop to set the image offsets, and then in outer



loop after the least squares fit. In practice, we required two (HRC, SBC) to four (WFC) cycles of the inner loop, and two of the outer loop to achieve convergence.

### 3.3 Low order terms

It is not possible to bootstrap all distortion coefficients from the dithered observations of programs 9028 and 9027. In particular the solution for the zeroth and first order terms in eq. 1 is degenerate. Instead, we must fix these terms using additional data. Our fitting procedure is to adopt  $a_{0,0}=0$  and  $b_{0,0}$ , and use the largest slew obtained with a given set of guide stars to determine the linear terms. The slews are given in terms of  $V_2, V_3$  which defines position in the HST focal plane. This method effectively sets the pixel scale and orientation of these two axes independently.

We compared the positions of stars in the 9018 program with cataloged star positions from the “Guide Star Catalogue II” (GSC2)<sup>3</sup> and USNO2<sup>4</sup> catalog as a check of the low order term for the WFC. An example is shown in Figure 4. A catalog of the 9018 field observed with the F555W filter was converted to  $X_{sky}, Y_{sky}$  positions using our initial fit and

matched with the published catalog after converting the RA, Dec positions to tangential plane offsets wrt to the nominal field center. The matching employs a simple linear fit to the  $X_{sky}, Y_{sky}$ . A total of 652 stars within 1.5" of ACS stars were matched with the GSC2 catalog and 195 stars within the same match radius were matched with the USNO2 (fig. 4). In addition we matched our WFC catalog with a catalog of an HST WFPC2 mosaic kindly made available by J. Anderson. We then performed linear fits in  $X_{sky}, Y_{sky}$  of the matched catalogs to constrain the linear terms, with the assumption that the non-ACS catalog coordinate system is correct. Unfortunately the results are not consistent between all catalog matches, indicating that there are small differences in the comparison catalog coordinate systems. Hence we can only constrain the  $X_{sky}, Y_{sky}$  scales of our system to be equal to within 0.04% and the skewness in the coordinate grid to be  $\sim 0.04^\circ$ . These limits allow the coordinate allow up to  $\sim 4$  pixels (0.2") difference from corner to corner of the WFC compared to a square tangential-plane grid. We intend to use WFC observations of the 9028 field obtained with a  $90^\circ$  roll-angle offset to provide a solution with tighter constraints. Those data were recently obtained by principal investigator Ivan King in program 9443, which was granted time as an HST calibration outsource proposal.

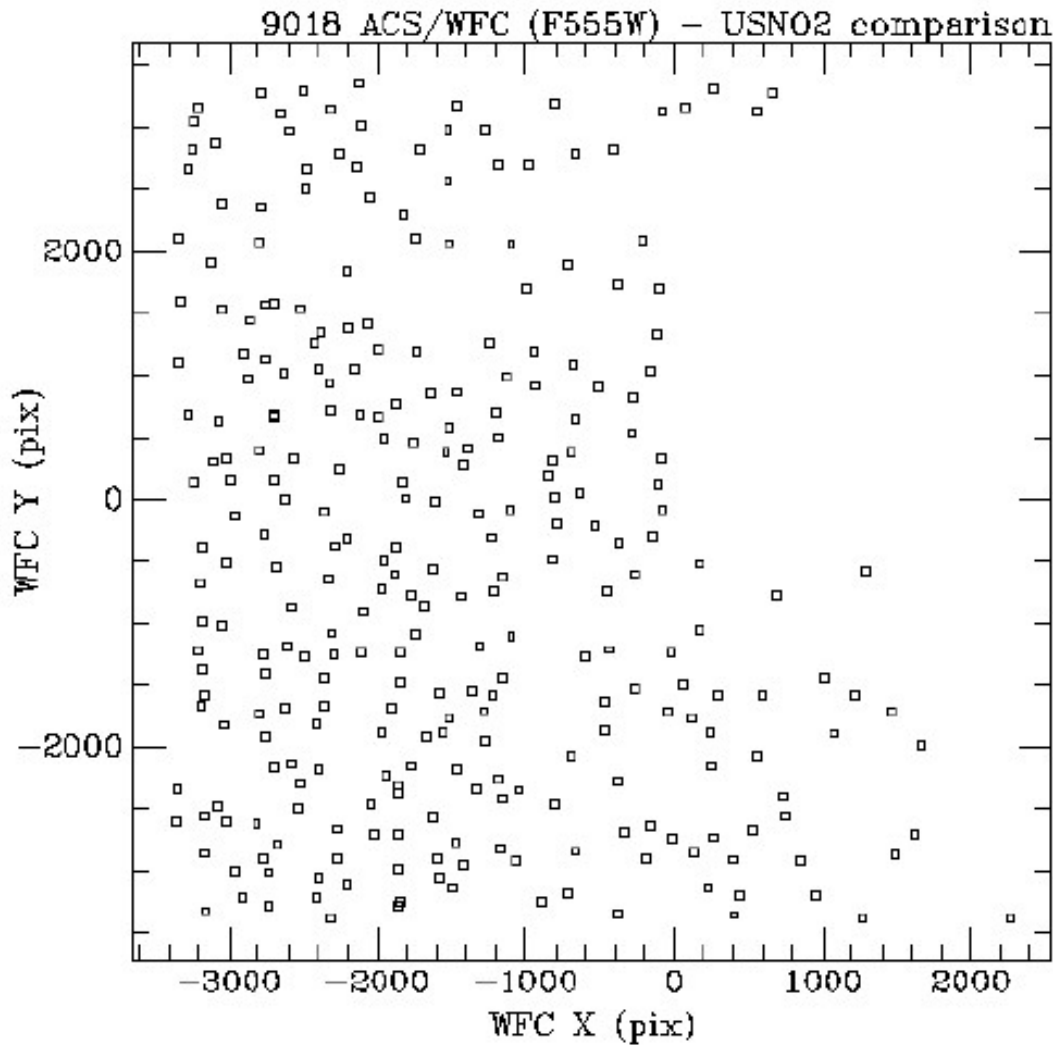


Figure 4 Stars matched in the 9018 field and the USNO2 catalog. Stars near the center of 47 Tuc are excluded from the USNO2 catalog, hence the empty area at upper left.

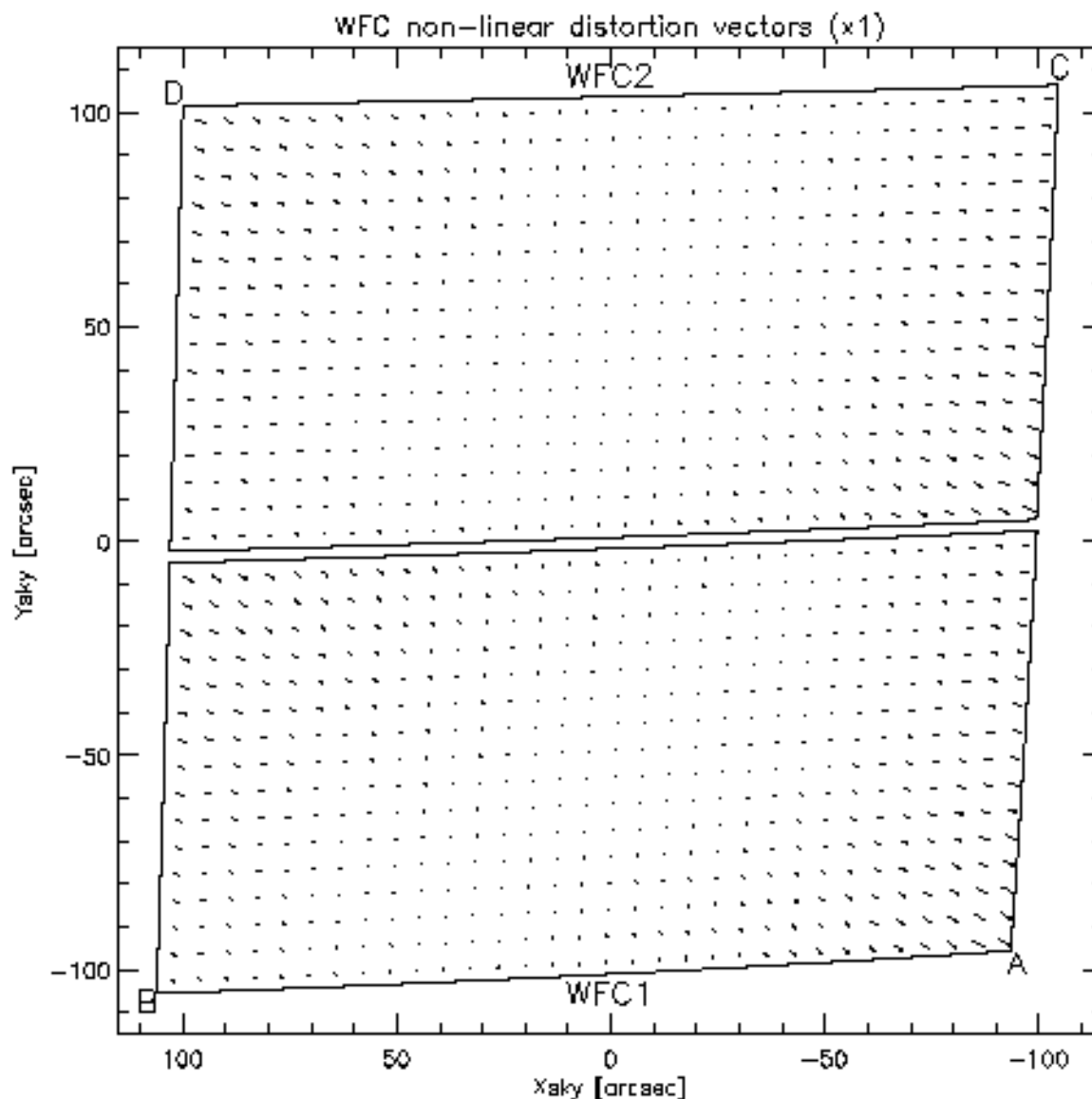


Figure 5. Non-linear portion of the geometric distortion of the WFC chips. The letters indicate the four read-out amplifiers.

We have constrained the linear terms of the HRC solution by matching the transformed  $X_{sky}, Y_{sky}$  of the WFC and HRC observations of the center of 47 Tuc. This solution will be updated when the improved WFC solution is obtained. The linear terms of the SBC solution will be set by matching the HRC and SBC catalogs of NGC6681.

## 4 RESULTS

The distortion in all ACS detectors is highly non-linear as illustrated in Fig. 5. We find that a quartic fit is adequate for characterizing the distortion to an accuracy much better than our requirement of 0.2 pixels over the entire field of view. Table 2 summarizes the rms of the fits to the various datasets. The WFC and HRC fits were all to F475W data as noted above.

Table 2. Summary of fit results

Camera	chip	pixel size	Filter	pointings	N	rms(x)	rms(y)	Notes
		[arcsec]				[pixels]	[pixels]	
WFC	1	0.05	F475W	20	112602	0.039	0.042	
WFC	2	0.05	F475W	20	79822	0.033	0.033	
WFC	1	0.05	F775W	10	35795	0.048	0.054	1
WFC	2	0.05	F775W	10	37796	0.042	0.041	1
HRC		0.025	F475W	20	78133	0.028	0.026	
HRC		0.025	F775W	13	31761	0.025	0.043	2
HRC		0.025	F220W	12	14836	0.112	0.108	2
SBC		0.03	F125LP	23	1032	0.086	0.074	
1 Coefficients held fixed to those found for WFC F475W.								
2 Coefficients held fixed to those found for HRC F475W.								

To check the wavelength dependence of the distortion we used data obtained with F775W (WFC and HRC) and F220W (HRC) from programs 9018 and 9019. We held the coefficients fixed and only fit the offsets in order to check whether a single distortion solution is sufficient for each detector. Table 2 shows that there is a marginal increase in the rms for the red data of the WFC, little or no increase in the fit rms for the red HRC data, but a significant increase in the rms using the UV data. An examination of the HRC F220W images reveals the most likely cause: the stellar PSF is elongated by  $\sim 0.1''$ . A similar elongation can also be seen in SBC PSFs (Fig. 1c). We attribute this to aberration in the optics of either the ACS M1 or M2 mirrors or the HST OTA. The aberration amounts to  $\sim 0.1$  waves at  $1600\text{\AA}$ , but is negligible relative to optical wavelengths hence it is not apparent in optical HRC images. Even the relatively poor HRC UV results are within our specification that the fit should be accurate to 0.2 pixels across the detector.

## 5 SUMMARY

We have described the algorithm we used to calibrate the geometric distortion of the ACS detectors. A fourth order fit to the F475W observations of 47 Tuc with WFC and HRC results in an rms of  $< \sim 0.05$  pixels. To this accuracy color terms are not necessary over optical observations. The rms of the fits is closer to  $\sim 0.1$  pixels in the UV as seen by the HRC and SBC detectors. This is likely to be in part due to aberration in the ACS optics or the HST Optical Telescope Assembly. Currently we are working to improve the accuracy of the linear terms of the solution using WFC data obtained of our primary calibration field at a different orientation.

## REFERENCES

<sup>1</sup> H.C. Ford, and the ACS Science Team, "The Advanced Camera for the Hubble Space Telescope," in *Space Telescopes and Instruments IV*, eds. P. Bely & J. Breckinridge, SPIE 2807, 184-196, 1996.

<sup>2</sup> R.L. Gilliland, et al., "A Lack of Planets in 47 Tucanae from a Hubble Space Telescope Search", *ApJ*, **545**, L47 – L51, 2000.

<sup>3</sup> Guide Star Catalogue II available from Space Telescope Science Institute, URL: <http://www-gsss.stsci.edu/gsc/gsc2/GSC2home.htm>.

<sup>4</sup> D. Monet, et al. 1998, *The PMM USNO-A2.0 Catalog*, U.S. Government Printing Office, Washington, 1998.